Spectral functions in nuclear matter

H. S. Köhler
Physics Department, University of Arizona, Tucson, Arizona 85721
(Received 18 February 1992)

Spectral functions are calculated from mean fields calculated both by Brueckner and by Botermans-Malfliet Green's function methods. Similarities and differences between the two methods are illustrated. Results are shown at normal nuclear matter density and zero temperature. Calculations are made by the separable phase-shift technique that was introduced earlier including the single-particle strength up to ~1700 MeV with (usually) less than 1% of the total strength missing. It is found that ~5% of the single particle strength lies above 500 MeV. Mean removal (centroid) energies of nucleons and occupation numbers are calculated by energy averaging over the spectral functions. The averages are also done in the extended quasiparticle approximation for the spectral function discussed in an earlier paper showing good agreement with the "exact" results. It is in fact shown that this approximation yields the same result for centroid energies as does Koltun's work which was based on an analysis of the linked cluster expansion. The total energy is calculated by Koltun's sum rule which involves an integration over the calculated (correlated) occupation numbers. The result compares favorably with the Brueckner energy which involves an integration over model (uncorrelated) occupation numbers.

PACS number(s): 21.65.+f, 21.10.Pc

I. INTRODUCTION

A new method to perform many-body calculations for nuclear matter was presented and applied in some previous publications [1,2]. The idea is to use the experimental phase shifts rather than a semiphenomenological potential model to calculate the effective interaction (i.e., the Brueckner K matrix or similarly defined object). This is possible by assuming that a matrix referred to as K_0, the diagonal elements of which are essentially the phase shifts, is separable in momentum space. The method has already been tested against potential-model calculations with no noticeable difference [1,2]. This concurs with the result that many-body calculations that have been made before with various potential models all agree, provided that the phase shifts are fitted equally. Quantities that were calculated by this new method involve mean fields, binding energy, occupation numbers, and spectral functions at zero as well as nonzero temperatures. Although the method (probably) can be refined, especially as regards the treatment of the tensor component of the force and the assumptions related to the sign change of the phase shifts (see Ref. [1]), the relative ease with which the method can be applied prompts us to pursue calculations by this method in its present form.

Although our main interest is to study nuclear dynamics at energies of several MeV as achieved in heavy ion collisions, this paper is devoted to ground-state nuclear matter. Calculations of spectral functions are shown that are more extensive and elaborate than in a previous paper [2]. The distribution of single-particle strength over a larger range of energy, as well as mean values of energy, etc., are calculated and described in the following sections. There are several papers on spectral functions published during the past few years using different methods [3–8]. Spectral functions are fundamental in describing nuclear correlations, experimentally accessible by $(e,e'p)$ experiments, and are of importance in relation to the EMC effect [9,10].

Most calculations in this publication are done by Brueckner theory. Some are done by Green's-function theory as formulated by Botermans and Malfliet [11]. Numerical comparisons between the two methods show agreements substantiating the formal comparison made in an earlier paper [12].

An approximation to the spectral function also introduced in this earlier paper (see also Ref. [13]) has interesting properties and establishes a link between the Bruekner and Green's-function theories. In this paper this *extended quasiparticle approximation (EQP)* is explored further and shows considerable agreement with the "exact" calculations.

Koltun [14] (see also Baranger [15]) showed an important theorem stating that the second-order Brueckner rearrangement energy does not contribute to the centroid of the removal energy of single particles from a specified state but only to its width. It is shown below that this theorem also follows from an application of the EQP approximation. Centroid energies calculated from the "exact" spectral functions also agree very closely with this theorem.

The paper is organized as follows. In Sec. II some basic formalism and definitions relevant for the calculations are presented, starting with Botermans and Malfliet [11] expressions for the mean field, etc., and continuing with the similar expressions in Brueckner theory. Section III contains the results of calculations using the separable phase-shift method with special emphasis on quantities derived from the spectral functions. Results are compared with those of the EQP approximation and comparisons with Koltun's work are made. A numerical comparison between the Brueckner method and the Green's-

function method in the formulation of Botermans and Malfliet is also shown. In Sec. IV a discussion and summary as well as suggestions for future work are presented.

II. FORMALISM

The quantum transport theory of Botermans and Malfliet [11] is based on the real-time Green's-function formalism of Schwinger, further developed by Kadanoff and Baym [16] and by Danielwicz [17,18]. This theory differs from the imaginary time formalism that does not allow the study of nonequilibrium (transport) properties [19]. Although the present study is only for nuclear matter in equilbrium, it is motivated by an interest to gain experience with this formalism for application to nuclear dynamics in general and heavy ion (HI) collisions in particular. It is also of interest to gain an understanding of possible differences from the Lehman-Galitskii formalism applied by other investigators [4,5,20].

In the present investigation the special emphasis is on spectral functions. Although the calculations will be restricted to zero temperature the theory is shown for temperature ≥ 0. The relevant equations are summarized below in general following the notations of Ref. [11]. The mean field is defined by

$$\Sigma^{(\pm)}(p)=-i\hbar\int\frac{d^4p'}{(2\pi\hbar)^4}[\langle\tfrac{1}{2}(\mathbf{p}-\mathbf{p}')|T^{(\pm)}(p+p')|\tfrac{1}{2}(\mathbf{p}-\mathbf{p}')\rangle_A g^{<}(p')+\langle\tfrac{1}{2}(\mathbf{p}-\mathbf{p}')|T^{<}(p+p')|\tfrac{1}{2}(\mathbf{p}-\mathbf{p}')\rangle_A g^{(\mp)}(p')] , \tag{1}$$

where $p=(\mathbf{p},\omega)$. The first term in Eq. (1) gives a first-order contribution to the mean field $\Sigma(p)$ in the effective interaction $T^{(\pm)}$ defined by

$$\langle\mathbf{p}|T^{(\pm)}(P)|\mathbf{p}'\rangle=\langle\mathbf{p}|v|\mathbf{p}'\rangle+(i\hbar)^2\int\frac{d^4p''\,d^4P''}{(2\pi\hbar)^8}\langle\mathbf{p}|v|\mathbf{p}''\rangle\frac{g^{>}(\frac{1}{2}P''+p'')g^{>}(\frac{1}{2}P''-p'')-g^{<}(\frac{1}{2}P''+p'')g^{<}(\frac{1}{2}P''-p'')}{\Omega-\Omega''\pm i\epsilon}$$
$$\times\langle\mathbf{p}''|T^{(\pm)}(P)|\mathbf{p}'\rangle(2\pi\hbar)^3\delta^3(\mathbf{P}-\mathbf{P}') , \tag{2}$$

where v is the N-N potential and P is the four-vector center-of-mass momentum with $P=(\mathbf{P},\Omega)$. The second term in Eq. (1) is of second order in $T^{(\pm)}$ because

$$\langle\mathbf{p}|T^{(\gtrless)}(P)|\mathbf{p}'\rangle=i\hbar\int\frac{d^4p''\,d^4p'''}{(2\pi\hbar)^8}\langle\mathbf{p}|T^{(+)}(P)|\tfrac{1}{2}(\mathbf{p}''-\mathbf{p}''')\rangle g^{\gtrless}(p'')g^{\gtrless}(p''')$$
$$\times\langle\tfrac{1}{2}(\mathbf{p}''-\mathbf{p}''')|T^{(-)}(P)|\mathbf{p}'\rangle(2\pi\hbar)^4\delta^4(P-p''-p''') . \tag{3}$$

In equilibrium we have

$$g^{<}(p)=-(1/i\hbar)S(p)n(\omega) ,$$
$$g^{>}(p)=(1/i\hbar)S(p)[1-n(\omega)] ,$$
$$n(\omega)=1/[e^{\beta(\omega-\mu)}+1] , \tag{4}$$

where $S(p)$ is the spectral function defined by

$$S(p)=i\hbar[g^{>}(p)-g^{<}(p)]$$
$$=i\hbar[g^{(+)}(p)-g^{(-)}(p)] \tag{5}$$

with

$$g^{(\pm)}(p)=\frac{1}{\omega-p^2/2m-\Sigma^{(\pm)}(p)\pm i\epsilon} \tag{6}$$

giving

$$S(p)=i\hbar\left[\frac{2i\,\mathrm{Im}\Sigma^{(+)}(p)}{[\omega-p^2/2m-\mathrm{Re}\Sigma^{(+)}(p)]^2+[\mathrm{Im}\Sigma^{(+)}(p)]^2}\right] , \tag{7}$$

satisfying the sum rule

$$\int S(p)d\omega=2\pi\hbar \tag{8}$$

for all values of $\mathbf{p}$. It should be noted that if Σ were independent of ω the sum rule is satisfied identically for any value of $\Sigma(\mathbf{p})$. For the sum rule to be satisfied in the general case it is evident that a relation between the ω dependences of the real and imaginary parts of Σ has to be satisfied. The dispersion relation is probably a sufficient condition although a proof of this is not known to exist.

There are several self-consistencies, all involving the mean field Σ, which have to be satisfied to solve the set of equations above. The most familiar may be the Brueckner-type self-consistency with Ω'' defined in terms of Σ (see below). A second self-consistency arises because of the ω dependence of the occupation numbers n defined by Eq. (4). The self-consistency that will be of special concern here relates to the spectral function defined in terms of the mean field in Eq. (7). For the first iteration it is natural to choose the spectral function in the quasiparticle (QP) approximation. Thus

$$S_{qp}(p)=2\pi\hbar Z(\mathbf{p})\delta(\omega-\omega_0) \tag{9}$$

with

$$\omega_0=p^2/2m+\mathrm{Re}\Sigma^{(+)}(\mathbf{p},\omega_0)\ ,$$
$$Z^{-1}(\mathbf{p})=\left[1-\frac{\partial \mathrm{Re}\Sigma^{(+)}(p)}{\partial\omega}\right]_{\omega=\omega_0}\ . \tag{10}$$

The ω integrations in Eqs. (1)–(3) are then trivial. A severe drawback with S_{qp} is that it normalizes to $2\pi\hbar Z$ rather than to $2\pi\hbar$ as in Eq. (8). We shall see below how this deficiency is remedied by the EQP approximation. At this point, however, we shall put $Z=1$, i.e., neglect the ω dependence of the mean field in Eq. (10), and refer to this as the quasiclassical (QC) approximation. One then finds

$$g^{(-)}(p)=\frac{1}{\omega-\omega_0-i\epsilon} \tag{11}$$

so that the mean field $\Sigma^{(+)}$ becomes

$$\Sigma^{(+)}(p)=\int\frac{d^3p'}{(2\pi\hbar)^3}\langle\tfrac{1}{2}(\mathbf{p}-\mathbf{p}')|T^{(+)}(\mathbf{p}+\mathbf{p}',\omega+\omega_0)|\tfrac{1}{2}(\mathbf{p}-\mathbf{p}')\rangle_A n(\mathbf{p}')$$
$$+\int\frac{d^3p'\,d^3p''\,d^3p'''}{(2\pi\hbar)^9}|\langle\tfrac{1}{2}(\mathbf{p}-\mathbf{p}')|T^{(+)}(\mathbf{p}''+\mathbf{p}''',\omega_0''+\omega_0''')|\tfrac{1}{2}(\mathbf{p}''-\mathbf{p}''')\rangle_A|^2$$
$$\times\frac{n(\mathbf{p}'')n(\mathbf{p}''')}{\omega+\omega_0'-\omega_0''-\omega_0'''+i\epsilon}(2\pi\hbar)^3\delta^3(\mathbf{p}+\mathbf{p}'-\mathbf{p}''-\mathbf{p}''')\ , \tag{12}$$

where the effective interaction now is

$$\langle\mathbf{p}|T^{(+)}(P)|\mathbf{p}'\rangle=\langle\mathbf{p}|v|\mathbf{p}'\rangle+\int\frac{d^3p''}{(2\pi\hbar)^3}\langle\mathbf{p}|v|\mathbf{p}''\rangle\frac{1-n(\frac{1}{2}\mathbf{P}+\mathbf{p}'')-n(\frac{1}{2}\mathbf{P}-\mathbf{p}'')}{\Omega-P^2/4m-p''^2/m-\mathrm{Re}\Sigma^{(+)}(\frac{1}{2}\mathbf{P}+\mathbf{p}'')-\mathrm{Re}\Sigma^{(+)}(\frac{1}{2}\mathbf{P}-\mathbf{p}'')+i\epsilon}$$
$$\times\langle\mathbf{p}''|T^{(+)}(P)|\mathbf{p}'\rangle\ . \tag{13}$$

These last two equations provide a first iteration from which the spectral functions can be calculated. In principle, one could continue the cycle of iterations by inserting these in Eqs. (1), (2), and (3). We shall return to this problem below in the discussions.

Equations (12) and (13) differ from the corresponding Brueckner equations:

$$V(p)=\int\frac{d^3p'}{(2\pi\hbar)^3}\langle\tfrac{1}{2}(\mathbf{p}-\mathbf{p}')|K(\mathbf{p}+\mathbf{p}',\omega+\omega_0)|\tfrac{1}{2}(\mathbf{p}-\mathbf{p}')\rangle_A n(\mathbf{p}')$$
$$+\int\frac{d^3p'\,d^3p''\,d^3p'''}{(2\pi\hbar)^9}|\langle\tfrac{1}{2}(\mathbf{p}-\mathbf{p}')|K(\mathbf{p}''+\mathbf{p}''',\omega_0''+\omega_0''')|\tfrac{1}{2}(\mathbf{p}''-\mathbf{p}''')\rangle_A|^2$$
$$\times\frac{[1-n(\mathbf{p}')]n(\mathbf{p}'')n(\mathbf{p}''')}{\omega+\omega_0'-\omega_0''-\omega_0'''-i\epsilon}(2\pi\hbar)^3\delta^3(\mathbf{p}+\mathbf{p}'-\mathbf{p}''-\mathbf{p}''')\ , \tag{14}$$

where

$$\langle\mathbf{p}|K(P)|\mathbf{p}'\rangle=\langle\mathbf{p}|v|\mathbf{p}'\rangle+\int\frac{d^3p''}{(2\pi\hbar)^3}\langle\mathbf{p}|v|\mathbf{p}''\rangle\frac{[1-n(\frac{1}{2}\mathbf{P}+\mathbf{p}'')][1-n(\frac{1}{2}\mathbf{P}-\mathbf{p}'')]}{\Omega-P^2/4m-p''^2/m-\mathrm{Re}V(\frac{1}{2}\mathbf{P}+\mathbf{p}'')-\mathrm{Re}V(\frac{1}{2}\mathbf{P}-\mathbf{p}'')+i\epsilon}$$
$$\times\langle\mathbf{p}''|K(P)|\mathbf{p}'\rangle\ . \tag{15}$$

The difference stems from the fact that intermediate hole states are included in the definition of T, while in the Brueckner K only the intermediate particle states are included. The relation between the two interactions is given by

$$\langle\mathbf{p}|T^{(+)}(P)|\mathbf{p}'\rangle=\langle\mathbf{p}|K(P)|\mathbf{p}'\rangle-\int\frac{d^3p''}{(2\pi\hbar)^3}\langle\mathbf{p}|K(P)|\mathbf{p}''\rangle$$
$$\times\frac{n(\frac{1}{2}\mathbf{P}+\mathbf{p}'')n(\frac{1}{2}\mathbf{P}-\mathbf{p}'')}{\Omega-P^2/4m-p''^2/m-\mathrm{Re}\Sigma^{(+)}(\frac{1}{2}\mathbf{P}+\mathbf{p}'')-\mathrm{Re}\Sigma^{(+)}(\frac{1}{2}\mathbf{P}-\mathbf{p}'')+i\epsilon}$$
$$\times\langle\mathbf{p}''|T^{(+)}(P)|\mathbf{p}'\rangle\ . \tag{16}$$

This is an exact relation between K and T. It is assumed that the energy denominator is the same in the two separate cases.

In Brueckner theory intermediate hole propagations are only contained in the second term in Eq. (14), often referred to as the Brueckner second-order rearrangement contribution to the mean field. Although the two theories are certainly different and the expressions for the first- and second-order mean-field terms differ, one finds that the *sum* of the two terms are in close agreement, i.e., $\Sigma \sim V$. This is easily seen [12] if one replaces the last T in Eq. (16) with K and inserts the resultant expression for T in Eq. (12). Up to second order in K one thus finds that $\Sigma^{(+)}(p)$ is equal to $V(p)$. This is very satisfactory, showing a close relation between the two theories. However, the sign of the imaginary part of the second-order term in Eq. (14) is *opposite* to that of Eq. (12) but equal to the representation utilized in other works [5,20,21]. This sign difference is also pointed out by Danielwicz [18]. For the zero-temperature calculation of spectral functions done in this paper this is of no consequence because the second-order term is zero for $k > k_F$ while the first-order term is zero for $k < k_F$. The two series are identical only to second order in K.

It is one purpose of this investigation to find the actual difference numerically as shown by results below. But most of the results in this paper will be by Brueckner theory. The reason is that, as we will find, the results related to removal energies are most easily discussed with reference to the Brueckner first- and second-order mean fields.

In the Brueckner mean field V defined by Eq. (14) the third-order rearrangement contribution is omitted because the Green's function Σ does not have a corresponding term in the QC approximation. In the QP approximation there would be such a term coming from the Z factors. However, only terms corresponding to the diagram of Fig. 1(c) would then be present while the diagram in Fig. 1(d) has no counterpart. This is directly related to the deficiency in the QP approximation mentioned above and explained as follows. Figure 1(c) corrects for the fact that a nucleon in state i interacts with another nucleon in state j which is a partially depleted hole state and Fig. 1(d) says that the missing strength is to be found in states b. The Z factors only say that the states are depleted but does not say where the strength is which amounts to the same as neglecting the diagram in Fig. 1(d).

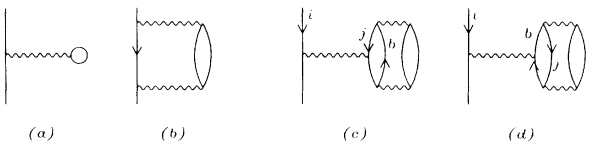

FIG. 1. Diagrammatic representation of first-, second-, and third-order contributions to the mean field (mass operator) discussed in text. Diagram (b) is often referred to as the Brueckner second-order rearrangement energy. The third-order diagram (c) can be considered as a correction to diagram (a) due to depletion of hole states caused by the correlation while (d) is a correction due to interaction with particle states created by the correlations. Only the first- and second-order diagrams are included in the mean field defined by Eq. (14). See text for discussions regarding the third-order diagrams.

The third-order rearrangement energy was included in previous papers [1,2]. However, it is not important for the conclusions of this paper. Its effect is mainly a renormalization effect of the first-order mean field by a factor of about 0.85 and a corresponding shift in quasiparticle energies. While it is not included by the QC approximation it will be included in the next iteration and in the EQP approximation discussed below.

All calculations presented in this paper will be at zero temperature. The spectral function is calculated from Eq. (7), in the case of Brueckner theory with Σ replaced by V. The occupation of hole states is then given by

$$\rho(\mathbf{p}) = \frac{1}{2\pi\hbar}\int_{-\infty}^{\mu} S(\mathbf{p},\omega)d\omega \ , \tag{17}$$

where μ is the chemical potential. The mean removal (or centroid) energy for a hole (particle) is given by

$$\begin{aligned} r_h(\mathbf{p}) &= -\frac{1}{2\pi\hbar\rho(\mathbf{p})}\int_{-\infty}^{\mu}\omega S(\mathbf{p},\omega)d\omega \ , \\ r_p(\mathbf{p}) &= -\frac{1}{2\pi\hbar[1-\rho(\mathbf{p})]}\int_{\mu}^{+\infty}\omega S(\mathbf{p},\omega)d\omega \ , \end{aligned} \tag{18}$$

where we used the fact that the sum of holes and particles equals 1.

An interesting approximation to the spectral function which goes beyond the quasiparticle approximation of Eq. (10) and referred to as the extended quasiparticle approximation is given by [12]:

$$\begin{aligned} S_{\mathrm{EQP}}(\mathbf{p},\omega) = 2\pi\hbar\delta(\omega-\omega_0)\left[1+\frac{\partial \mathrm{Re}V(\mathbf{p},\omega)}{\partial\omega}\right]_{\omega=\omega_0} \\ -\mathcal{P}\frac{2\mathrm{Im}V(\mathbf{p},\omega)}{(\omega-\omega_0)^2} \ , \end{aligned} \tag{19}$$

where $\mathcal{P}$ refers to a principal value integration. In the second term $(\omega-\omega_0)^{-2}$ should be interpreted as

$$[d/d\omega'(\omega-\omega')]_{\omega'=\omega_0} \ .$$

In the previous publication [12] this approximation was discussed with reference to Brueckner theory. It is obtained by an expansion around the quasiparticle peak with $\mathrm{Im}V \ll \mathrm{Re}V$. It has several interesting features. It satisfies the sum rule expressed by Eq. (8) which is *not* satisfied in the quasiparticle approximation. The strength missing in the QP approximation is contained in the second term of Eq. (19). Notice, however, that the first term in this equation is not identical to the QP approximation. The EQP approximation is especially studied to use with the Brueckner theory in which $\mathrm{Im}V^{(1)}(\mathbf{p},\omega)=0$ for $\omega<\omega_F$ while $\mathrm{Im}V^{(2)}(\mathbf{p},\omega)=0$ for $\omega>\omega_F$ with $V^{(1)}$ and $V^{(2)}$ being the first- and second-order terms of the mean field in the Brueckner approximation equation (14). Using the dispersion relations between the real and imaginary parts of each of these fields one finds, inserting

S_{EQP} into Eq. (17),

$$\rho^a(\mathbf{p})=n(\mathbf{p})\left[1+\frac{\partial \mathrm{Re}V^{(1)}(\mathbf{p},\omega)}{\partial\omega}\right]_{\omega=\omega_0} +[1-n(\mathbf{p})]\left[\frac{\partial \mathrm{Re}V^{(2)}(\mathbf{p},\omega)}{\partial\omega}\right]_{\omega=\omega_0}, \tag{20}$$

and this is exactly the Brueckner-approximation for the occupation numbers [12,22].

To find the mean removal energy from Eq. (18) in the same approximation one first notices that

$$r_h(\mathbf{p})=-\frac{\int_{-\infty}^{\mu}\omega S(\mathbf{p},\omega)d\omega}{\int_{-\infty}^{\mu}S(\mathbf{p},\omega)d\omega} =-\omega_0-\frac{\int_{-\infty}^{\mu}(\omega-\omega_0)S(\mathbf{p},\omega)d\omega}{\int_{-\infty}^{\mu}S(\mathbf{p},\omega)d\omega}\ ; \tag{21}$$

using the EQP approximation for the spectral function one then finds

$$r_h^a(\mathbf{p})=-\omega_0+\frac{\mathcal{P}\int_{-\infty}^{\mu}[2\,\mathrm{Im}V(\mathbf{p},\omega)/(\omega-\omega_0)]d\omega}{\int_{-\infty}^{\mu}S(\mathbf{p},\omega)d\omega}\ . \tag{22}$$

Using the dispersion relation and noticing the relations pointed out above Eq. (20) one then finds the following expressions for the centroid energy for hole (particle) removal in the EQP approximation:

$$r_h^a(\mathbf{p})=-\omega_0+\frac{\mathrm{Re}V^{(2)}(\mathbf{p},\omega_0)}{\rho(\mathbf{p})}\ , \qquad r_p^a(\mathbf{p})=-\omega_0+\frac{\mathrm{Re}V^{(1)}(\mathbf{p},\omega_0)}{1-\rho(\mathbf{p})}\ . \tag{23}$$

(The last of these two equations is found by replacing the limits of integration above with $\mu\to+\infty$.) It is indeed satisfactory that this very compact result agrees exactly with the result of Koltun [14] in his diagrammatic analysis of Brueckner theory. It illustrates the usefulness of the EQP approximation. It should be noticed that for hole states below the Fermi surface $\rho(\mathbf{p})\sim 1$ which leads to the sometimes used statement that "the Brueckner second-order rearrangement energy does not contribute to the centroid energy (for hole states) but only to the width." Koltun discusses this point.

This summarizes the formalism needed for the presentation and discussion of the results presented in this paper. Some relations referring to the Koltun sum rule are shown in Sec. III, Pt. 3.

III. RESULTS OF CALCULATIONS

1. Some computational details

The calculations of the reaction matrix was done as in recent publications [1,2]. The phase-shift model M1 was used [1]. However, only the states with $J\leq 2$ were included while in previous work all states with $J\leq 5$ were used. Because this investigation is concerned with correlations as exhibited by the spectral functions and the states of higher angular momenta have much smaller correlations they were not included. As in previous work the mean field used in defining the propagator in Eq. (15) contained not V but only the first-order mean field $V^{(1)}$ calculated to be self-consistent in model M1 (see Ref. [1]). However, the computer program was rewritten to better accommodate the calculation of the ω dependence of the fields. The momentum mesh was further increased from 0.1 to 0.2 fm^{-1} with some small sacrifice in accuracy. Each calculation of the mean field at a fixed momentum $\mathbf{p}$ as a function of 120 values of ω from -280 to 1722 MeV took 87 s CPU on the YMP Cray at the San Diego Supercomputer Center. The spectral functions are strongly peaked as a function of ω especially around the Fermi surface. In order to accurately do the ω integrations, the spectral functions were therefore calculated in a separate program from the mean fields after putting them on a 1-MeV mesh obtained by interpolation from the $\sim$13-MeV mesh specified above.

The real part of the second-order mean field was calculated from the dispersion relation connecting it with the imaginary part. This could in principle also be done for the first-order but is not as straightforward because of the background terms. The dispersion relation was for reasons of technical convenience still used to calculate parts of the K matrix that involve principal value integrations. It should be noted that the sum rule expressed by Eq. (8) *probably* relies on the dispersion relation between the real and imaginary parts to be satisfied. We are not aware of any proof of this statement but the proof in the case of the EQP approximation does certainly rely on this.

2. Numerical results

The spectral functions were calculated at 11 values of the momentum $\mathbf{p}$ between 0 and 2.25 fm^{-1} (in units of $\hbar$). The normalization was satisfied for most momenta to within 1% although for one momentum as much as 4% is missing. The last column in Table I lists $N(\mathbf{p})$ as the integral in Eq. (8) in units of $2\pi\hbar$. The missing strength may be located above our upper limit $\omega\sim 1720$ MeV. The lower limit for a pole to appear is twice the potential energy at the bottom of the Fermi sea which is well covered within the range of ω's that is used in the calculations (see the previous section). The convergence to full strength at the upper range of ω's, is, however, quite slow as shown in Fig. 2. It is seen that almost 5% of the strength lies above 500 MeV. It is to be expected that the precise distribution of strength is tied to the potential model that one uses. A larger short-ranged repulsion give even slower convergence. In our phase-shift model this relates to increased repulsive phase-shifts at high energy. It should also be realized, however, that the "nucleons only model" that we use becomes unphysical at these high energies; internal degrees of freedom of the nucleons, particle production, etc., would set in.

Occupation numbers $\rho(\mathbf{p})$ are calculated from Eq. (17) and shown in Table I. Comparing with the EQP (or Brueckner) approximation $\rho^a(\mathbf{p})$ calculated from Eq. (20), one sees a difference with the approximate being

TABLE I. Units are in MeV and fm.

p	ω_0	$r_h(\mathbf{p})$	$r_h^a(\mathbf{p})$	$V^{(1)}(\mathbf{p},\omega_0)$	$V^{(2)}(\mathbf{p},\omega_0)$	$\rho(\mathbf{p})$	$\rho^a(\mathbf{p})$	$N(\mathbf{p})$
0.0	−74.1	104.6	114.7 (107.8)	$-107.7+i0$	$33.7+i24.7$	0.87	0.83	0.99
0.23	−73.5	103.5	113.4 (106.6)	$-107.7+i0$	$33.1+i23.7$	0.87	0.83	1.00
0.45	−67.8	96.6	106.2 (99.6)	$-103.6+i0$	$31.8+i19.3$	0.87	0.83	1.00
0.68	−62.1	86.2	94.9 (88.9)	$-98.2+i0$	$26.8+i15.0$	0.87	0.82	1.00
0.90	−50.7	70.4	79.0 (73.0)	$-89.4+i0$	$22.3+i8.9$	0.85	0.79	0.99
1.12	−38.5	53.2	60.8 (55.4)	$-81.2+i0$	$16.9+i4.3$	0.82	0.76	0.98
1.35	−24.4	34.4	39.7 (35.6)	$-73.1+i0.5$	$11.3+i1.3$	0.77	0.74	0.98
1.57	−7.1	79.7	69.7	$-65.2+i2.1$	$7.0+i0.1$	0.06	0.11	1.00
1.80	12.4	101.1	76.4	$-59.1+i6.3$	$4.3+i0$	0.03	0.05	0.97
2.03	35.1	113.4	100.0	$-52.7+i12.2$	$2.9+i0$	0.01	0.02	0.96
2.25	61.7	125.8	111.2	$-45.4+i16.8$	$2.0+i0$	0.01	0.01	0.99

$\sim 0.04 \rightarrow 0.06$ too small when going from the bottom towards the top of the Fermi sea. At the Fermi surface it is 0.03 smaller. Similar differences are seen for states above the Fermi momentum, but the approximate values are now as expected larger to make up for the larger depletion below the surface. Similar results for occupation numbers calculated by the approximate method was already shown in Fig. 5 of Ref. [3]. That calculation was independent in that the computer program was rewritten to accommodate the full ω dependence. Nevertheless it agrees closely with the present result. The only numerically noticeable difference is at the Fermi surface. For states just above we now find $\rho^a(\mathbf{p})=0.13$ instead of the previously found value $=0.21$ so that the discontinuity (in the EQP approximation) now is 0.61 instead of the previously found value of 0.52. Some difference is in fact to be expected between these new calculations and the previous. In the previous calculations the quasiparticle energy defined by Eq. (10) did not include $V^{(2)}$ but only $V^{(1)}$ so that the derivatives with respect to ω in Eq. (20) are calculated at different values of ω in the two cases (see also Sec. III, Pt. 3).

Figure 3 shows that the spectral functions are peaked closely to the quasiparticle values ω_0 (indicated by short vertical lines) except for the smallest values of momentum $\mathbf{p}$ where the width is very large and the spectral function actually is double peaked. The centroid (or removal) energies $r_h(\mathbf{p})$ are indicated by the arrows in Fig. 3. They are seen to be shifted down in energy from ω_0 especially for states above the Fermi momentum so that some of the latter actually lie below those that are *in* the Fermi sea. This was also pointed out by Koltun [14]. It was shown above that this shift according to both Koltun's analysis and the EQP approximation should be given by Eq. (23) and this is listed in Table I as $r_h^a(\mathbf{p})$. One sees that this approximation in general gives $\sim 10\%$ too large removal energies. The values within parentheses are obtained by setting $\rho(\mathbf{p})=1$ in Eq. (23) for states below the Fermi surface and these actually agree better with the numerical results r_h. Thus the nu-

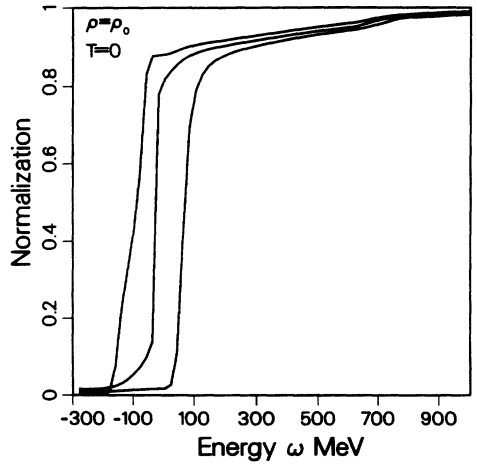

FIG. 2. The normalization integral equation (8) as a function of the upper limit ω for the three momenta $\mathbf{p}=0.0$, 1.35, and 2.25 fm^{-1} (from left to right). Notice the slow convergence due to the high-energy strength of the spectral function caused by the short-ranged correlations.

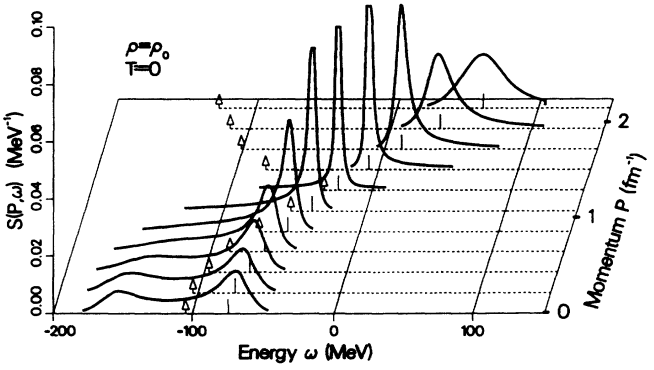

FIG. 3. The spectral function as a function of $(\mathbf{p},\omega)$. The short vertical lines indicate the quasiparticle energy ω_0 defined by Eq. (10). The arrows indicate the removal energy $r_h(\mathbf{p})$ defined by Eq. (18). The three functions at, below, and above the Fermi momentum 1.35 fm^{-1} are strongly peaked and are cut off. The actual maxima are from left to right 0.08, 0.16, and 0.13 MeV^{-1}.

merical result agrees quite closely with the statement made above in Sec. II saying that the *Brueckner second-order rearrangement energy does not contribute to the mean removal energy.*

3. Koltun's sum rule

The total energy of a system is related to the spectral function by

$$E=4\frac{1}{2}\int_{-\infty}^{\mu}d\omega\int_{-\infty}^{+\infty}\frac{d^3p}{(2\pi\hbar)^3}[p^2/2m-\omega]S(\mathbf{p},\omega)\ . \tag{24}$$

This relation is in nuclear physics known as Koltun's sum rule [14]. The factor 4 is due to spin isospin degeneracy. Using our previous notations Eq. (24) can, after performing the ω integration, be rewritten as

$$E=4\frac{1}{2}\int_{-\infty}^{+\infty}\frac{d^3p}{(2\pi\hbar)^3}[p^2/2m-r_h(\mathbf{p})]\rho(\mathbf{p})\ . \tag{25}$$

With the previously calculated values of $r_h(\mathbf{p})$ and $\rho(\mathbf{p})$ shown in Table I one finds a binding energy per article

$$\text{B.E.}/A=17.4\ \text{MeV}\ .$$

Replacing $r_h(\mathbf{p})$ and $\rho(\mathbf{p})$ in Eq. (25) with $r_h^a(\mathbf{p})$ and $\rho^a(\mathbf{p})$, respectively, i.e., using the EQP approximation one finds

$$\text{B.E.}/A(\text{EQP})=19.5\ (17.2)\ \text{MeV}\ .$$

The value within parentheses comes from using the parenthesized $r_h^a(\mathbf{p})$ in Table I and is in remarkable agreement with the "exact" value above. It was already noted above that these $r_h^a(\mathbf{p})$ agree better with the exact values $r_h(\mathbf{p})$. Setting $\rho(\mathbf{p})\sim 1$ in Eq. (23) (for r_h) is anyway not inconsistent for states below the Fermi surface as Koltun also discusses. A related effect is that of the third-order rearrangement term that was neglected in the present calculations. It is actually proportional to the depletion $1-\rho(\mathbf{p})$. Its inclusion would actually decrease the removal energies by about 10% and this is roughly the difference here.

The sum rule involves a sum over actual occupation numbers in the correlated medium. An alternate (Brueckner) expression for the energy involves a sum over model occupation numbers and is given by

$$E=4\int_0^{p_F}\frac{d^3p}{(2\pi\hbar)^3}[p^2/2m+\tfrac{1}{2}V^{(1)}(\mathbf{p},\omega_0)]n(\mathbf{p}) \tag{26}$$

with $n(\mathbf{p})=1$ below the Fermi surface and zero otherwise. With $V^{(1)}$ given in Table I one finds the expression to give

$$\text{B.E.}/A=20.0\ \text{MeV}\ ,$$

i.e., substantially larger than the binding energies above. The high-energy extrapolation of the phase shifts with all $J\leq 5$ that is used in model M1 were normalized to give a binding energy

$$(\text{B.E.}/A)_{J\leq 5}=15.5\ \text{MeV}\ ,$$

as described in Ref. [1]. However, in the present work only states with $J\leq 2$ are considered. The contribution from the states with $2<J\leq 5$ is at normal density -1.2 MeV as found from the end of Sec. III in Ref. [1] giving

$$(\text{B.E.}/A)_{J\leq 2}=16.7\ \text{MeV}$$

which compares favorably with the result 17.4 MeV above. But why does the expression in Eq. (26) yield a binding energy which is 3.3 MeV larger than the earlier (identical) calculation in Ref. [1]. The answer is that in Eq. (26) the mean field is defined at $\omega=\omega_0$ but in Ref. [1] the Brueckner self-consistent energy ω_B is defined by

$$\omega_B=p^2/2m+\text{Re}V^{(1)}(\mathbf{p},\omega_B)$$

so that two calculations are in fact *not* identical. The difference between the two ω's is the Brueckner second-order rearrangement energy which is positive. Figure 6 shows that $V^{(1)}$ increases with decreasing ω and this explains the discrepancy.

4. Effect of hole propagation

In Fig. 4 the solid curve shows a spectral function calculated by the Brueckner method, i.e., with V defined by Eq. (14). The dotted line shows the corresponding result by the Malfliet method, i.e., with the $\Sigma^{(+)}$ defined by Eq. (12). We remind the reader that the latter includes hole propagations in the effective interaction. The calculation is done at $\mathbf{p}=0$ and, because this is a deep hole state, the difference between the two methods should therefore be at its largest here. Some difference is noticed but the hole strengths have on the whole the same shape. The quasiparticle energies are different in the two cases as shown by the vertical lines but are rather meaningless quantities here because of the large width. The mean field for the two separate cases is shown in Fig. 5 by the solid and dot-

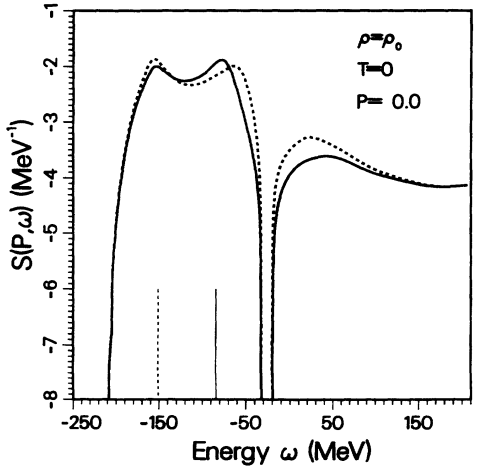

FIG. 4. Logarithmic plot of the spectral function as a function of ω at $\mathbf{p}=0$. The solid curve is from Brueckner theory while the dotted curve is from Malfliet's theory as defined in Sec. II.

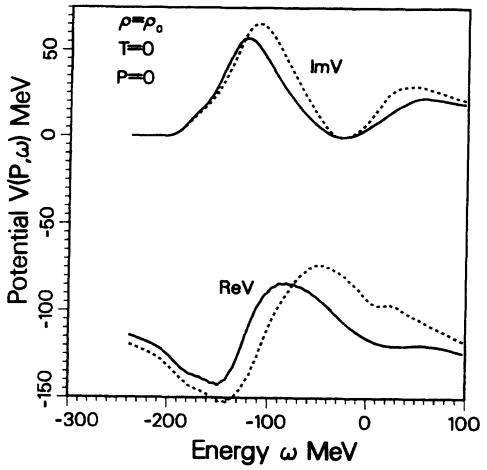

FIG. 5. Real and imaginary parts of the mean field by Brueckner and Malfliet methods are shown by solid and dotted curves respectively and are used for getting the spectral functions in Fig. 4.

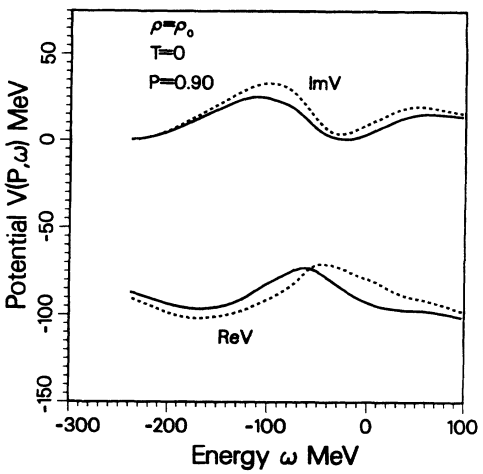

FIG. 7. This curve is similar to Fig. 5 but is at $\mathbf{p}=0.90$ fm^{-1}.

ted lines, respectively. The imaginary parts both go to zero at the Fermi energy as is to be expected and the general shapes of the curves are the same. The curves for real parts cross each other at about the quasiparticle energy. The relative agreement between these curves should be contrasted with the significant difference between the first- and second-order terms compared individually in Fig. 6. It should be noticed that the Brueckner (solid) curve for $\mathrm{Im}V^{(1)}$ is zero below the Fermi surface while the same is true for $\mathrm{Im}V^{(2)}$ above the Fermi surface, a fact that led to the simple relations derived in the EQP approximation above. On the other hand, no such simple relation exists with regard to first- and second-order parts of $\mathrm{Im}\Sigma$, in the figure shown by the dotted lines $\mathrm{Im}\Sigma^{(1)}$ and $\mathrm{Im}\Sigma^{(2)}$, respectively. The imaginary part of $\Sigma^{(1)}$ is not even qualitatively similar to the imaginary part of $V^{(1)}$. So the two methods give quite different results at this level of comparison. The agreement is so much closer when looking at the *sums* of first- and second-order fields. It should be noted that for $\omega=\omega_F$ one should have $\mathrm{Im}\Sigma^{(1)}=-\mathrm{Im}\Sigma^{(2)}$. This is satisfied to a good accuracy as seen from Fig. 5 and is a good test of the numerical accuracy of the calculations and in agreement with the Brueckner result. It is of course expected because the lifetime of a particle at the Fermi energy should be infinite at zero temperature. The agreement between the two methods is somewhat closer at a larger momentum exemplified by Fig. 7 at $\mathbf{p}=0.90$ fm^{-1} although the $\mathrm{Im}\Sigma$ potential is not exactly zero here at the Fermi surface as it should be. It was already shown that the two methods agree exactly to second order in K so that any difference is of third order and involve hole-hole interactions [12]. These are included in the Brueckner second-order rearrangement term $V^{(2)}$ but only to a lower order from which the difference arises.

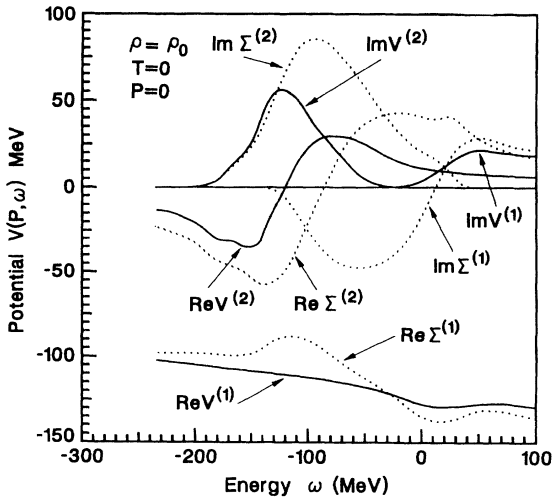

FIG. 6. These curves are similar to those in Fig. 5 but here the first- and second-order terms are plotted separately.

One may argue that for the Green's-function formalism used here, the real-time formalism is awkward as compared to that of some other works [5,20,21] at zero temperature. But an important purpose of the present work is to gain experience with the real-time formalism applicable to nonequilibrium systems, where the other formalisms fail as discussed repeatedly in past publications [11,16,18,19].

IV. SUMMARY AND DISCUSSIONS

A main purpose of this continuing investigation (with previous work referenced above) is the exploration of the kinetic theory in the Green's-function formulation given by Botermans and Malfliet. It is believed to be important to do this in a systematic fashion by first establishing contact in the equilibrium limit with the more studied method of Brueckner. Some formal comparison was made in an earlier paper [12] and also discussed above in Sec. II. The numerical comparisons found in Sec. III essentially substantiate the earlier formal results. It is found that the hole propagations missing in the

Brueckner K matrix are *essentially* contained in the Brueckner second-order rearrangement energy. There is some numerical difference between the two methods as regards the total mean field. This is of course expected. The difference that was pointed out above with reference to Figs. 4–7 is of course subject to some numerical uncertainty. It is felt, however, that the difference is real and outside the limits of numerical accuracy. The Green's-function method with the hole state propagator in the effective interaction should in principle be the most accurate of the two.

It is noted that the sign of the imaginary part of the second-order term in Eq. (14) is opposite to that of other works [5,20,21] using the Lehmann-Galitskii formalism. As pointed out above this is of no consequence for the present $T=0$ calculations. The difference in sign between the chronological and retarded single-particle formalisms at zero temperature was pointed out by Danielewicz [18]. The numerical differences for $T>0$ are not known. The real-time formalism, however, has an advantage of being simpler to apply for this case and of course for nonequilibrium situations where the other formalisms do not apply or become awkward.

A complete solution of the Green's-function many-body problem requires a self-consistent iteration involving spectral functions as seen from Eqs. (1), (2), etc. The comparison discussed above was made in a first iteration using the quasiparticle approximation. Using the computed spectral functions in the next iteration would lead to a much more computer intensive calculation involving numerical integrations over the ω variable. This may still be a possible task using the separable phase-shift method utilized in this paper. It was also found, however, that all tests of the relatively simple EQP approximation suggests this to be a more than adequate approximation to be used for a second iteration. This will be explored further in a forthcoming publication. The third-order rearrangement energy [shown by the diagrams in Figs. 1(c) and 1(d)] is absent in Eqs. (13) and (14) but will, as an example, be included by this second iteration. It was already pointed out above that this energy does not qualitatively affect the results but it does have quantitative effects resulting from energy shifts and this has an implication for example in relation to Koltun's sum rule as discussed in Sec. III, Pt. 3. It is a direct consequence of correlations and is often referred to as a renormalization due to depletion of states. The first iteration of Eqs. (1), (2), etc., with the uncorrelated QC approximation for the spectral function does not contain this renormalization but it is generated by this first iteration, i.e., contained in a second iteration. This of course has been well known since the early days of Brueckner theory and with discussions of a fully renormalized theory (see, for example, Refs. [23–25]). The Green's-function method appears to provide a scheme to accomplish such a renormalization consistently.

The EQP approximation is found to be quite good at normal density and zero temperature. If either of these variables are increased, the imaginary part of the mean field increases and this approximation may become less useful. Its range of validity therefore still remains to be explored (numerically).

The EQP approximation was furthermore found to provide a direct proof of Koltun's results on centroid energies as was discussed above in Sec. III, Pt. 2. This is not surprising in view of the fact that this approximation for the spectral function establishes a link between the Green's-function and Brueckner methods as shown in Ref. [12]. Koltun's work was based on a diagrammatic analysis while our results were derived directly from the EQP approximation for the spectral function. In a following contribution in this series of papers it will be shown that this approximation also is very helpful for clarifying the connection between higher-order Brueckner and Green's-function methods in particular as regards the definition of single-particle (-hole) propagator energies.

ACKNOWLEDGMENTS

It is a pleasure to thank Professor Rudi Malfliet for the many discussions from which this work has evolved. It is also a pleasure to thank Professor Pawel Danielewicz for illuminating discussions. This work was supported in part by the National Science Foundation, under Grant No. PHY-9106357 and by NATO Collaborative Research Grant No. CRG 900145 with Professor Rudi Malfliet. Most of the calculations were made on the Cray Y-MP8/864 at the San Diego Supercomputer Center under Acct. No. UOA-206.

[1] H. S. Köhler, Nucl. Phys. **A529**, 209 (1991).
[2] H. S. Köhler, Nucl Phys. **A537**, 64 (1992).
[3] O. Benhar, A. Fabrocini, and S. Fantoni, Nucl. Phys. **A505**, 267 (1989).
[4] B. E. Vonderfecht, W. H. Dickhoff, A. Polls, and A. Ramos, Phys. Rev. C **44**, 1265 (1991).
[5] A. Ramos, A. Polls, and W. H. Dickhoff, Nucl. Phys. **A503**, 1 (1989).
[6] Fred de Jong and Rudi Malfliet, Phys. Rev. C **44**, 998 (1991).
[7] P. Grangé, J. Cugnon, and A. Lejune, Nucl. Phys. **A473**, 365 (1987).
[8] M. Baldo, I. Bombaci, G. Giansiracusa, U. Lombardo, C. Mahaux, and R. Sartor, University of Liege, Belgium, Report No. ULG-PNT-91-5-P, 1991.
[9] A. E. L. Dieperink and G. A. Miller (unpublished).
[10] S. Shlomo and G. M. Vagradov, Phys. Lett. B **232**, 19 (1989).
[11] Wim Botermans and Rudi Malfliet, Phys. Rep. **198**, 115 (1990).
[12] H. S. Köhler and R. Malfliet (unpublished).
[13] W. D. Kraeft, D. Kremp, W. Ebeling, and G. Röpke, *Quantum Statistics of Charged Particle Systems* (Akademie-Verlag, Berlin, 1986).

[14] D. S. Koltun, Phys. Rev. **9**, 484 (1974); Phys. Rev. Lett. **28**, 182 (1972).
[15] Michel Baranger, Nucl. Phys. **A149**, 225 (1970).
[16] L. P. Kadanoff and G. Baym, *Quantum Statistical Mechanics* (Benjamin, New York, 1962).
[17] P. Danielewicz, Ann. Phys. (N.Y.) **152**, 239 (1984).
[18] P. Danielewicz, Ann. Phys. (N.Y.) **197**, 154 (1990).
[19] M. Marinaro, Phys. Rep. **137**, 81 (1986).
[20] V. Bernard and C. Mahaux, Phys. Rev. C **23**, 888 (1981).
[21] C. Mahaux, P. F. Bortignon, R. A. Broglia, and C. H. Dasso, Phys. Rep. C **120**, 1 (1985).
[22] J.-P. Jeukenne, A. Lejeune, and C. Mahaux, Phys. Rep. C **25**, 83 (1976).
[23] Baird H. Brandow, Rev. Mod. Phys. **39**, 771 (1967).
[24] H. S. Köhler, Nucl. Phys. **A204**, 65 (1973).
[25] H. S. Köhler, Phys. Rep. C **18**, 217 (1975).